



Industrial Lubrication and Tribology

Research on thermal-fluid-structure coupling of valve plate pair in an axial piston pump with high pressure and high speed

Zhanling Ji,

Article information:

To cite this document:

Zhanling Ji, (2018) "Research on thermal-fluid-structure coupling of valve plate pair in an axial piston pump with high pressure and high speed", *Industrial Lubrication and Tribology*, Vol. 70 Issue: 6, pp.1137-1144, <https://doi.org/10.1108/ILT-04-2017-0102>

Permanent link to this document:

<https://doi.org/10.1108/ILT-04-2017-0102>

Downloaded on: 02 September 2018, At: 05:24 (PT)

References: this document contains references to 19 other documents.

To copy this document: permissions@emeraldinsight.com

The fulltext of this document has been downloaded 20 times since 2018*

Access to this document was granted through an Emerald subscription provided by emerald-srm:464870 []

For Authors

If you would like to write for this, or any other Emerald publication, then please use our Emerald for Authors service information about how to choose which publication to write for and submission guidelines are available for all. Please visit www.emeraldinsight.com/authors for more information.

About Emerald www.emeraldinsight.com

Emerald is a global publisher linking research and practice to the benefit of society. The company manages a portfolio of more than 290 journals and over 2,350 books and book series volumes, as well as providing an extensive range of online products and additional customer resources and services.

Emerald is both COUNTER 4 and TRANSFER compliant. The organization is a partner of the Committee on Publication Ethics (COPE) and also works with Portico and the LOCKSS initiative for digital archive preservation.

*Related content and download information correct at time of download.

Research on thermal-fluid-structure coupling of valve plate pair in an axial piston pump with high pressure and high speed

Zhanling Ji

Institute of Mechanics, Chinese Academy of Sciences, Beijing, China and
School of Automation Science and Electrical Engineering, Beihang University, Beijing, China

Abstract

Purpose – High pressure and high speed of the axial piston pump can improve its power density, but they also deteriorate the thermal-fluid-structure coupling effect of the friction pairs. This paper aims to reveal the coupling mechanism of the pump, for example, valve plate pair, by carrying out research on multi-physics field coupling.

Design/methodology/approach – Considering the influences of temperature on material properties and thermal fluid on structure, the thermal-fluid elastic mechanics model is established. A complete set of fast and effective thermal-fluid-structure coupling method is presented, by which the numerical analysis is conducted for the valve plate pair.

Findings – According to calculations, it is revealed that the temperature and pressure evolution laws of oil film with time, the pressure distribution law of the fluid, stress and displacement distribution laws of the solid in the valve plate pair. In addition, the forming history of the wedge-shaped oil film and mating clearance change law with rotational speed and outlet pressure in the valve plate pair are presented.

Originality/value – For an axial piston pump operating under high speed, high pressure and wide temperature range, the multi-physics field coupling analysis is an indispensable means and method. This paper provides theoretical evidence for the development of the pump and lays a solid foundation for the research of the same kind of problem.

Keywords Axial piston pump with high-pressure and high-speed, Thermal-fluid elastic deformation, Thermal-fluid-structure coupling, Valve plate pair

Paper type Research paper

Nomenclature

dp_r, dp_θ, dp_z = radial, tangential and axial volume force increment, N/m^3 ;
 $d\bar{p}_r, d\bar{p}_\theta, d\bar{p}_z$ = radial, tangential and axial surface force increment, N/m^2 ;
 du^*, dv^*, dw^* = tiny virtual radial, tangential and axial displacement increment, $m/rad/m$;
 u_r, u_θ, u_z = radial, tangential and axial speed, $rad/s, m/s$;
 \mathbf{u} = speed vector;
 $\{f\}$ = displacement vector at some point, rad, m ;
 r, θ, z = coordinate axes;
 N_i = shape function;
 $[N]$ = shape function matrix;
 $\{T\}^e$ = temperature vector, K ;
 dP_r, dP_θ, dP_z = radial, tangential, axial concentrated force increment, N ;
 $[B]$ = geometry matrix;
 $[D]$ = elastic matrix;
 R', T', Z' = radial, tangential, axial unit mass force, N/kg ;

T = temperature, K ;
 T_0 = reference temperature, K ;
 R_p = piston distribution radius, m ;
 ρ = density, kg/m^3 ;
 η = oil viscosity, $Pa.s$;
 η_0 = oil viscosity at temperature T_0' , $Pa.s$;
 $d\{\varepsilon\}$ = total strain increment;
 $d\{\varepsilon\}_e$ = elastic strain increment;
 $d\{\varepsilon\}_T$ = thermal strain increment;
 $d\sigma_r, d\sigma_\theta, d\sigma_z$ = radial, tangential, axial stress increment, Pa ;
 $d\varepsilon_r^*, d\varepsilon_\theta^*, d\varepsilon_z^*$ = virtual radial, tangential, axial strain increment;
 $d\tau_{r\theta}, d\tau_{\theta z}, d\tau_{zr}$ = shear stress increment in $r\theta, \theta z, zr$ planes, Pa ;
 $d\gamma_{r\theta}^*, d\gamma_{\theta z}^*, d\gamma_{zr}^*$ = virtual shear strain increment in $r\theta, \theta z, zr$ planes;
 $\{\delta^*\}^e$ = virtual nodal displacement vector of an element, m ;
 $d\{\delta^*\}^e$ = virtual nodal displacement increment vector of an element, m ;

The current issue and full text archive of this journal is available on Emerald Insight at: www.emeraldinsight.com/0036-8792.htm



Industrial Lubrication and Tribology
70/6 (2018) 1137–1144
© Emerald Publishing Limited [ISSN 0036-8792]
[DOI 10.1108/ILT-04-2017-0102]

The authors would like to acknowledge the support of the National Key Basic Research Program of China (Grant No.2014CB046403) and Project funded by China Postdoctoral Science Foundation (Grant No. 2017M611010).

Received 18 April 2017
Revised 14 December 2017
Accepted 14 January 2018

| | |
|---------------------------|---|
| $d\{\delta\}^e$ | = nodal displacement vector of an element, m; |
| $\{\epsilon\}$ | = strain vector; |
| $d\{\tilde{\epsilon}\}_T$ | = initial strain at each iteration; |
| $d\{\tilde{\sigma}\}_T$ | = initial stress at each iteration, Pa; |
| $\{\alpha\}$ | = thermal expansion array, $10^{-6}/\text{K}$; |
| α | = thermal expansion coefficient, $10^{-6}/\text{K}$; and |
| ω | = relative angular speed, rad/s. |

Introduction

A higher rotational speed of the axial piston pump is required in aircraft for achieving adequate power density. The speed can reach 9,000 rpm, even 16,000 rpm. Thus, the heat induced by high pressure and high speed increases during the operating process. This heat makes the oil viscosity change drastically, thereby changing the bearing, sealing and lubricating characteristics. In addition, the heat and high pressure increase the local deformation in the core components. The inadequate lubrication and inconsistent deformation make the friction pairs seriously wear. These further increase the oil leakage and generated heat and make the oil film formation more difficult. Therefore, as one of the key friction pairs, there is an urgent need to study valve plate pair from the perspective of multi-physics field coupling.

Many scholars have studied the axial piston pump from many aspects. For the oil film of the valve plate pair, Frnaeo (1961) used the proposed method under constant film thickness assumption, and Yamaguchi first used the numerical method by considering the influence of the wedge-shaped film (Yamaguchi, 1966) and conducted further research by adding an unsteady item in Reynolds equation (Yamaguchi, 1984). Pan *et al.* (1989) carried out some research studies by using the finite difference method. Mandal *et al.* (2012) studied the effects of flow inertia and valve-plate geometry on the axial piston pump. Bergada *et al.* (2012) discussed how barrel film thickness and barrel dynamics of an axial piston pump depend on oil pressure and temperature. Richardson *et al.* (2017) pointed out that the motion of the floating valve plate directly affected the lubricating pressures between valve plate and cylinder block. For the sea water axial piston, Yang *et al.* (2015) studied the influence of pre-compression angle, friction coefficient and clearance on the torque. Xu *et al.* (2017a, 2017b) analyzed the influence of dimensional and geometrical errors on the cylinder block tilt (Xu *et al.*, 2017a, 2017b) and studied hydro-mechanical losses of various friction pairs of the pump.

Ivantysynova and team carried out numerous studies on the axial piston pump. For the piston pair, Ivantysynova and Huang (2002, 2002) first considered the elasto-hydro-dynamic effect, and Pelosi and Ivantysynova (2009) first presented the thermal-fluid-structure coupled model. In 2016, Shang and Ivantysynova (2016) used the fluid structure and thermal interaction model to investigate the complex fluid behavior of the cylinder block/valve plate interface, and Chacon and Ivantysynova (2016) studied the impact of the elastic deformation due to pressure and thermal loadings of the end case/housing on the performance of the cylinder block/valve plate interface, but for the fluid, only oil film was considered. In addition, for slipper pair or external gear machine, research on

thermo-elasto-hydro-dynamic lubrication has been conducted (Tang *et al.*, 2017; Hashemi *et al.*, 2017; Thiagrajan *et al.*, 2015; Dhar and Vacca, 2015).

By analyzing and summarizing the literature, for the valve plate pair of the axial piston pump with high pressure and high speed, with the increase in rotational speed and operating pressure, high-speed shear flow and high-pressure difference flow make transient flow and viscous heating more obvious. Therefore, future research should be focused on the transient analysis and thermal-fluid-structure coupling.

Therefore, we consider the effects of temperature, high speed and high pressure for conducting transient thermal-fluid-structure coupling research for the valve plate pair.

Problem formulation

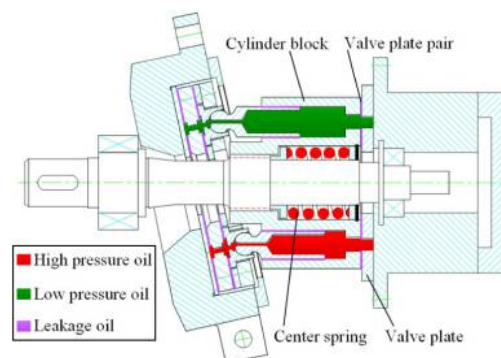
The flow distributor mechanisms are mainly composed of valve plate, cylinder block and center spring, as shown in Figure 1. Valve plate is used to insulate oil, distribute oil and bear the load from the cylinder block, which is fixed at the rear end of the pump housing by a side pin. Cylinder block rotates at a constant speed, which is driven by a spline of the rotational shaft. When the pump starts, the relative motion exists between cylinder block and valve plate, and the oil in the piston chambers together with the spring presses the cylinder block toward the valve plate. Lubrication film is immediately formed and a certain gap is maintained between the two, thereby avoiding direct contact friction.

In the valve plate pair, under high speed and high pressure, temperature rises of valve plate and cylinder block and oil in them, and deformations of valve plate and cylinder block are larger. They are not completely the same at different locations, resulting in higher stress and wedge-shaped clearance, and interactions exist among them. These usually cause a series of consequences, involving unsteady operation of the pump, insufficient pumping oil pressure and partial wear. Moreover, the consequences determine efficiency, operation performances, reliability and service life of the pump. Therefore, research on thermal-fluid-structure coupling in the valve plate pair is imperative.

Thermal-fluid elastic mechanics model

Suppose that the valve plate pair is loaded by volume force (such as temperature load), surface force (such as fluid pressure) and concentrated force and its research region is

Figure 1 Axial piston pump with high pressure and high speed



discretized as finite elements. For each element e , according to the incremental virtual work principle, the equation is established as follows:

$$\begin{aligned} & \sum_e \int_V (d\sigma_r d\varepsilon_r^* + d\sigma_\theta d\varepsilon_\theta^* + d\sigma_z d\varepsilon_z^* + d\tau_{r\theta} d\gamma_{r\theta}^* \\ & + d\tau_{\theta z} d\gamma_{\theta z}^* + d\tau_{zr} d\gamma_{zr}^*) dV \\ & - \sum_e \int_V (dp_r du^* + dp_\theta dv^*) dV - \sum_e \int_V (dp_z dw^*) dV \\ & - \sum_e \int_{S_\sigma} (d\bar{p}_r du^* + d\bar{p}_\theta dv^* + d\bar{p}_z dw^*) dS \\ & - \sum_e (dP_r du^* + dP_\theta dv^* + dP_z dw^*) = 0 \end{aligned} \quad (1)$$

In an element, using the virtual nodal displacement $\{\delta^*\}^e$, the virtual displacement $\{f^*\}$ at any point is expressed as:

$$\{f^*\}^e = [N]\{\delta^*\}^e \quad (2)$$

The virtual strain $\{\varepsilon^*\}$ is defined as:

$$\{\varepsilon^*\} = [B]\{\delta^*\}^e \quad (3)$$

In the elastic regions, the total strain increment is decomposed as:

$$d\{\varepsilon\} = d\{\varepsilon\}_e + d\{\varepsilon\}_T \quad (4)$$

Taking the derivative of $\{\varepsilon\}_e = [D]^{-1}\{\sigma\}$ yields:

$$d\{\varepsilon\}_e = \frac{d[D]^{-1}}{dT}\{\sigma\}dT + [D]^{-1}d\{\sigma\} \quad (5)$$

Taking the derivative of $\{\varepsilon\}_T = \{\alpha\}\{T - T_0\}$ yields:

$$d\{\varepsilon\}_T = \frac{d\{\alpha\}}{dT}\{T - T_0\}dT + \{\alpha\}dT \quad (6)$$

Substituting equations (5) and (6) into equation (4) yields:

$$d\{\varepsilon\} = \frac{d[D]^{-1}}{dT}\{\sigma\}dT + [D]^{-1}d\{\sigma\} + \frac{d\{\alpha\}}{dT}\{T - T_0\}dT + \{\alpha\}dT \quad (7)$$

Multiplying equation (7) by $[D]$ at the two ends and then arranging it yields:

$$d\{\sigma\} = [D](d\{\varepsilon\} - d\{\tilde{\varepsilon}\}_T) \quad (8)$$

where $d\{\tilde{\varepsilon}\}_T = \left(\{\alpha\} + \frac{d[D]^{-1}}{dT}\{\sigma\} + \frac{d\{\alpha\}}{dT}\{T - T_0\}\right)dT$.

The deduction of equations (1)-(8) can be referred to Rao's works (Rao, 1982).

For every element, substituting equations (2), (3) and (8) into equation (1) yields:

$$\begin{aligned} & \left(\int_V d\{\delta\}^T [B]^T [D]^T [B] d\{\delta^*\}^e dV - \int_V (d\{\tilde{\varepsilon}\}_T)^T [D]^T [B] d\{\delta^*\}^e dV \right) \\ & - \int_V \{dp\}^T [N] d\{\delta^*\}^e dV - \int_{S_\sigma} \{d\bar{p}\}^T [N] d\{\delta^*\}^e dS - \{dP\}^T [N] d\{\delta^*\}^e = 0 \end{aligned} \quad (9)$$

Transposing and arranging equation (9) yields:

$$[k]^e d\{\delta\}^e = \{dF\}_T^e + \{dF\}_p^e + \{dF\}_\bar{p}^e + \{P\}^e \quad (10)$$

where:

$$\begin{aligned} [k]^e &= [B]^T [D] [B], \\ \{dF\}_T^e &= \int_V [B]^T [D] (d\{\tilde{\varepsilon}\}_T) dV, \\ \{dF\}_p^e &= \int_V [N]^T \{dp\} dV, \\ \{dF\}_\bar{p}^e &= \int_{S_\sigma} [N]^T \{d\bar{p}\} dS, \\ \{P\}^e &= [N]^T \{dP\}. \end{aligned}$$

The global stiffness equation is modeled according to element stiffness equation (10), thereby achieving the corresponding displacements and stresses.

Numerical calculation and result discussion

Research case

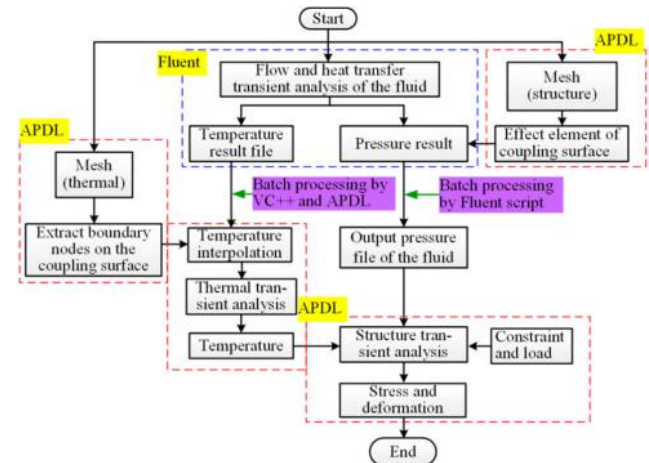
To study the influence of different outlet pressures and rotational speeds on coupling characteristics of valve plate pair, outlet pressure $p = 30$ MPa and speed $n = 12,000$ r/min are selected as the basic case. Other cases studied are as follows: outlet pressure $p = 25$ MPa and speed $n = 9,000$ r/min; outlet pressure $p = 30$ MPa and speed $n = 9,000$ r/min; outlet pressure $p = 32$ MPa and speed $n = 9,000$ r/min; and outlet pressure $p = 30$ MPa and speed $n = 12,000$ r/min.

Thermal-fluid-structure coupling flow

To carry out the coupling analysis for the valve plate pair, a complete set of fast and effective thermal-fluid-structure coupling method is put forward. Its flowchart is shown in Figure 2, and the detailed steps are as follows:

- The calculations of temperature and pressure on the fluid-structure coupling interfaces are accomplished by Fluent, and then the batch processing for the temperature result is accomplished by VC++ and APDL.
- The boundary nodes are extracted on the fluid-structure coupling interfaces by APDL, and temperature of the nodes is interpolated with that of the corresponding nodes in the previous step.
- The transient thermal analysis in the structure is carried out by APDL.
- The equivalent elements are obtained on the fluid-structure coupling interfaces by APDL.

Figure 2 Thermal-fluid-structure coupling flowchart



- Pressure of the equivalent elements in the previous step are processed in batches by Fluent script.
- The temperature in the third step and the pressure in the fifth step are loaded into the structure model according to load step, constraints and other loads are added, and the transient structure analysis is accomplished.

In the method, Fluent with user-defined function is applied for fluid calculation, and ANSYS Parametric Design Language is adopted for solid calculation. Therefore, compared with the system coupling module of ANSYS Workbench platform and mesh-based parallel code coupling interface, it has the incomparable advantages, such as no special restrictions for the research objects, flexible solution and other settings and high computation efficiency.

Results and discussion

Fluid field analysis

In the valve plate pair, pressure distribution and temperature distribution of the fluid at 0.125 s are shown in Figures 3 and 4, respectively. In Figure 3, the pressure is higher at regions connected with the oil discharge port; when the fluid in a piston passes through Damping Groove 1, oil pressure instantaneously rises at the location. In Figure 4, the temperature of the entire oil film and part of the piston coupling walls is higher.

Figure 5 shows the pressure distribution of the oil film in the valve plate pair when the pump works for different time. By the analysis for Figure 5, the following conclusions can be drawn:

- The highest pressure of the oil film sometimes exceeds the rated pressure. The value is closely related to the relative position among pistons and damping grooves. For example, when a piston passes through Damping Groove

Figure 3 Pressure distribution of the fluid at 0.125 s in the valve plate pair (30 MPa and 12,000 r/min)

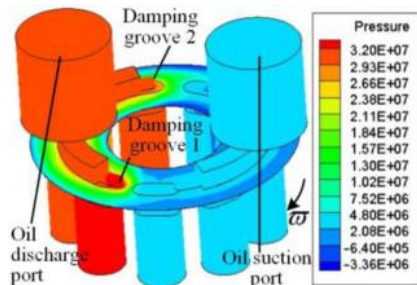
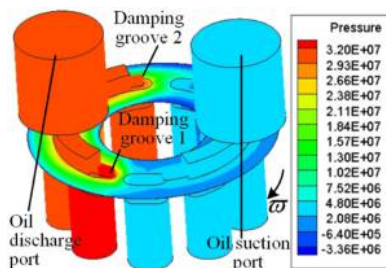


Figure 4 Temperature distribution of the fluid at 0.125 s in the valve plate pair (30 MPa and 12,000 r/min)



1, because of the outflow oil blocked by the groove, instantaneous pressure ripple occurs.

- When a piston passes through Damping Groove 2, because of high-pressure fluid in the piston chamber at the time, the pressure at part of Transition Region 2 is also high.
- In the oil discharge region, a higher pressure gradient exists along the radial direction.
- Compared to the other oil suction region, at Damping Groove 3, because of the transition from high pressure to low pressure and increasing outflow area, with the rotation of the cylinder block, the pressure greatly varies.
- With the rotation of the cylinder block, the position among cylinder holes and oil discharge port is constantly changing, and high pressure distribution is also slightly different and varies between Damping Grooves 1 and 3.

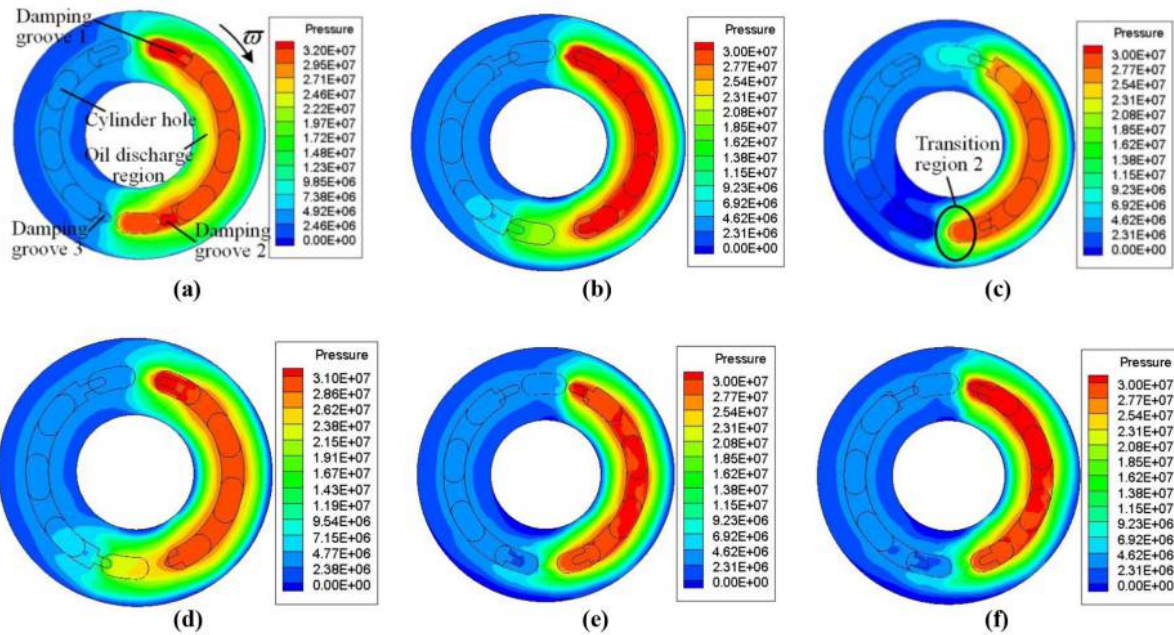
When the pump works for different time, temperature distributions of the oil film in the valve plate pair are shown in Figure 6. The time history of temperature rise of oil film can be seen in Figure 6.

- At the initial working stage, the temperature near Damping Groove 1 increases sharply because of the damping effect. The temperature is higher near the outer edges of the oil film and the oil discharge port in the oil discharge region and Damping Groove 3.
- With the rotation of the cylinder block, because of the high-temperature oil leaving from the oil discharge region, temperature value and relative high temperature area near Damping Groove 3 even exceed those near Damping Groove 1.
- After a period of time, the temperatures of oil film among adjacent cylinder holes and valve plate gradually increase. But the locations of relatively high temperature region always change with the rotation of the cylinder block. And their numbers also increase from 1 to 3. After that, even in the oil suction region, relative high temperature occurs at the corresponding locations, and their temperatures gradually decrease along the rotation direction of the cylinder block.
- Because of the decreasing pressure and the rotation of the cylinder block, near Damping Groove 2, a heart-shape lower temperature region occurs, whose area gradually shrinks.
- With the increasing operation time, along the rotation direction of the cylinder block, the temperature of oil film continuously increases until the temperature of the entire oil film is almost high.
- After 0.01 s, the temperature distribution shapes are basically stable, i.e. except the locations near oil suction port, oil discharge port and Damping Groove 1, the temperature of oil film is high. Because of the low-temperature oil entering from the oil suction region, the temperature near Damping Groove 1 is relatively lower.

Thermal analysis for the solid

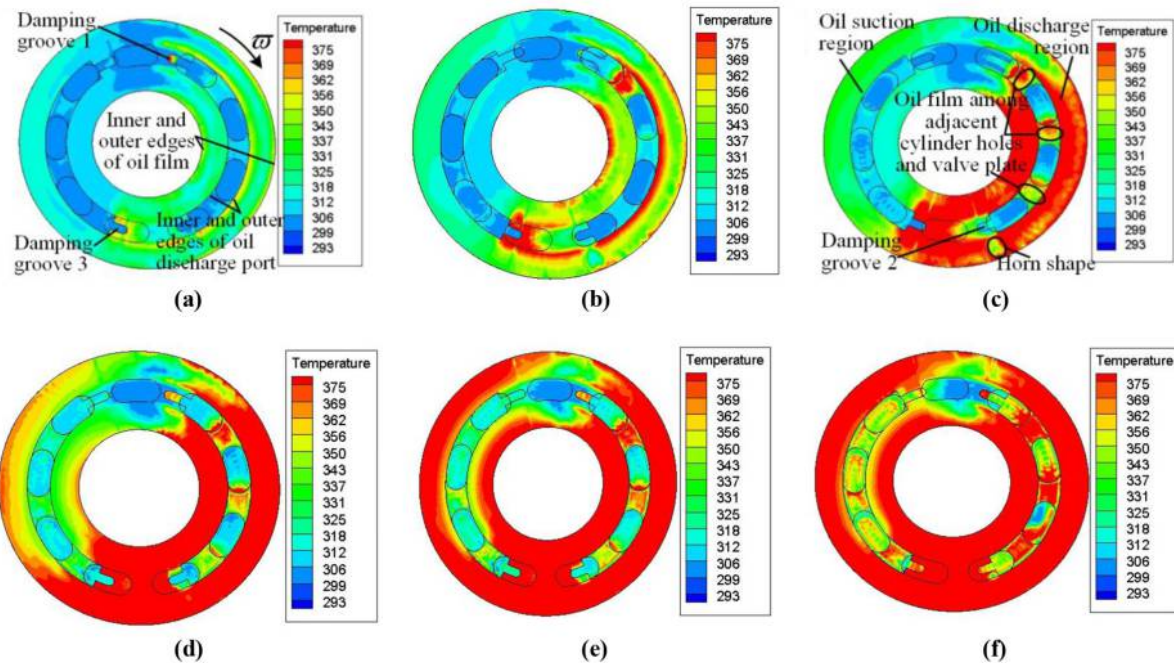
When the pump works until 0.125 s, the temperature distributions of the valve plate and the cylinder block are shown in Figures 7 and 8, respectively. From Figures 7 and 8, it is seen that the high temperature area is larger, and the temperature

Figure 5 Pressure distribution of the oil film in the valve plate pair when the pump works for different time



Notes: (a) 0.00025 s; (b) 0.001 s; (c) 0.00125 s; (d) 0.0015 s; (e) 0.005 s; (f) 0.125 s (30 MPa and 12,000 r/min)

Figure 6 Temperature distribution of the oil film in the valve plate pair when the pump works for different time



Notes: (a) 0.0005 s; (b) 0.001 s; (c) 0.002 s; (d) 0.005 s; (e) 0.01 s; (f) 0.125 s (30 MPa and 12,000 r/min)

distribution laws of the valve plate and cylinder block are in accordance with those of the oil film, which suggests that the temperature interpolation from the fluid to the structure is right.

Thermal-fluid elastic analysis for the solid

When the pump works until 0.125 s, the von Mises stress distributions of the valve plate and the cylinder block are shown in Figures 9 and 10, respectively. In Figure 9, the higher stress

Figure 7 Temperature distribution of the valve plate at 0.125 s (30 MPa and 12,000 r/min)

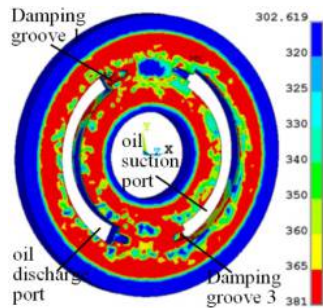


Figure 8 Temperature distribution of the cylinder block at 0.125 s (30 MPa and 12,000 r/min)

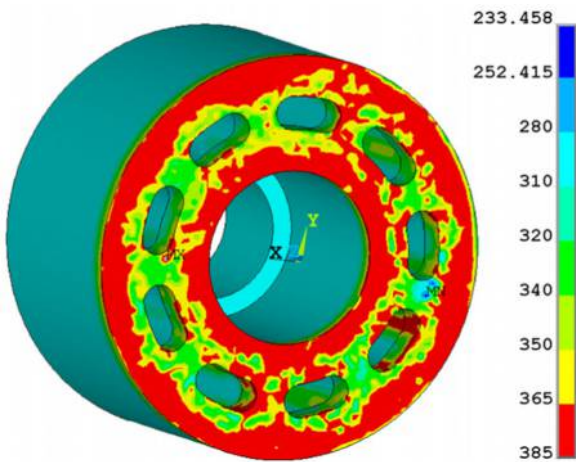
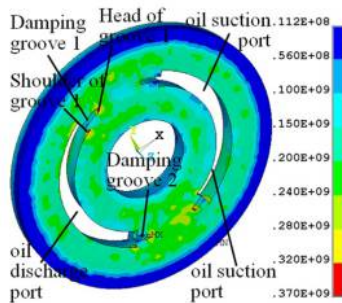


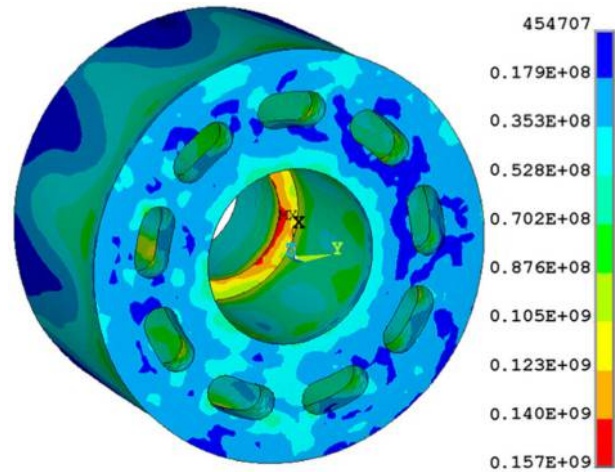
Figure 9 von Mises stress of the valve plate at 0.125 s (30 MPa and 12,000 r/min)



is located at the heads of Damping Grooves 1, 2 and 3, some shoulders of oil discharge port and oil suction port. The maximum stress is over 370 MPa. At this time, it is noted whether the value exceeds the yield limit or the fracture limit of the material. In Figure 10, The maximum stress occurs at the changed cross section of the internal surface of the cylinder block, which also is the dividing line of the constraint. The maximum stress is 157 MPa.

When the pump works until 0.125 s, the axial deformation contours of the valve plate and the cylinder block are shown

Figure 10 von Mises stress of the cylinder block at 0.125 s (30 MPa and 12,000 r/min)



in Figures 11 and 12, respectively. Overall, the axial deformation of the valve plate is smaller than that of the cylinder block. The axial deformation sizes are different at the oil discharge side and the oil suction side of the cylinder block. Between the cylinder block and the valve plate, the clearance increases at the oil discharge side, whereas the clearance changes little or decreases at the oil suction side. The wedge-shaped clearance forms are shown in Figure 13.

The mating clearance

To investigate the mating clearance changing with time, two pairs of nodes on the front surface of the valve plate and the bottom surface of the cylinder block are selected. Under different rotational speeds and different outlet pressures, at these locations, the curves of the mating clearance change versus time are shown as Figures 14 and 15, respectively. By the analysis for them, the following conclusions are drawn:

Figure 11 Axial deformation of the valve plate when the pump works until 0.125 s

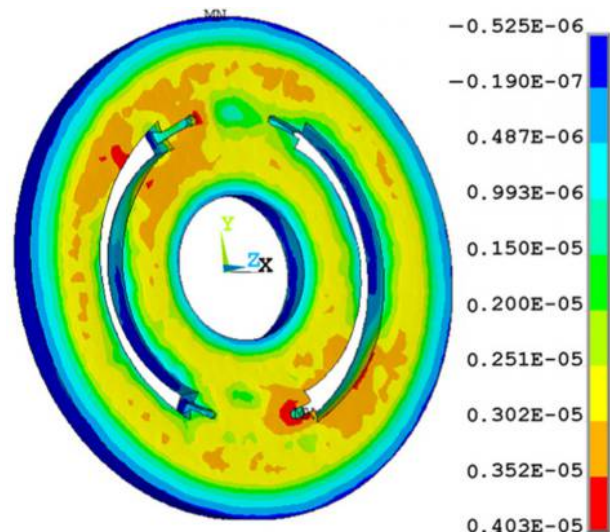


Figure 12 Axial deformation of the cylinder block when the pump works until 0.125 s

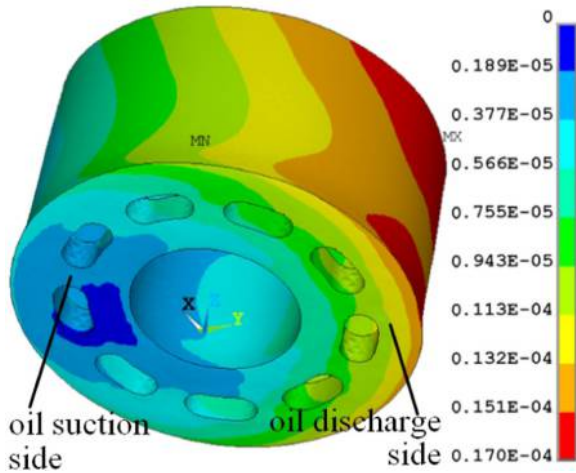


Figure 13 Wedge-shaped clearance between cylinder block and valve plate ($\times 150$)

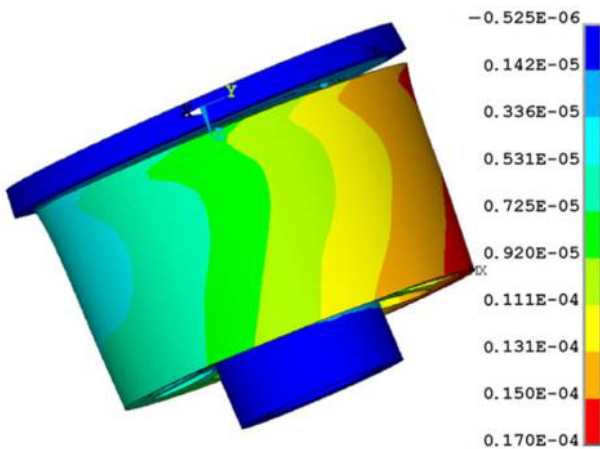


Figure 14 Mating clearance change curves versus time under different rotational speed

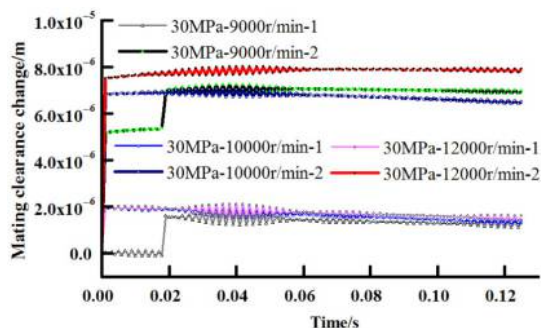
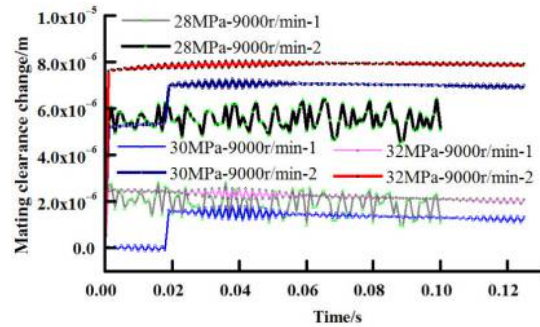


Figure 15 Mating clearance change versus time curves under different outlet pressures



- Compared with rotational speed, the influence of outlet pressure on mating clearance is larger, such as 28 and 30MPa (Figure 15).
- Under high pressure and high speed, the mating clearances at the majority places increase, but the increasing sizes are different and sometimes also decrease at some local regions, such as 30 MPa-9,000 r/min, thereby forming wedge-shaped clearance.
- Compared with other cases, under the case of 28 MPa-9,000 r/min, the changing magnitude of mating clearance is larger because the area of low temperature oil is larger under 28 MPa, whereas over 30 MPa, the entire oil film is almost a high temperature region, and the deformation induced by the pressure is also larger.
- In general, the higher the pressure, the higher the speed and the more the clearance increase.
- With the increase in operation time, the overall change trend of mating clearance is from rapidly increasing to smaller amplitude of oscillation.

Conclusions

Using the fast and effective multi-physics field coupling method proposed, the numerical analysis on the valve plate pair is conducted, and the main conclusions are as follows:

- When a piston passes through Damping Groove 1 or 2, instantaneous pressure ripple of the oil film and the fluid in the valve plate pair occurs. The value is closely related to the relative position among pistons and damping grooves. High pressure region of the oil film varies between Damping Grooves 1 and 3.
- After 0.01 s, the temperature distribution shapes of the oil film are basically stable, and the temperature of the entire oil film is almost high.
- Compared with other cases, under the case of 28 MPa-9,000 r/min, the changing magnitude of mating clearance is larger.
- The forming history of wedge-shaped clearance is from rapidly increasing to smaller amplitude of oscillation.

For research on the generated heat and the deformation of an axial piston pump working under high speed, high pressure and wide temperature range, the multi-physics field coupling analysis is an indispensable means and method, and it is extended to more application areas, such as the wet multidisc

brake of a heavy vehicle, the pantograph-catenary system and the vehicle-track system of a high-speed train.

References

- Bergada, J.M., Davies, D.L., Kumar, S. and Watton, J. (2012), "The effect of oil pressure and temperature on barrel film thickness and barrel dynamics of an axial piston pump", *Meccanica*, Vol. 47 No. 3, pp. 639-654.
- Chacon, R. and Ivantysynova M. (2016), "An investigation of the impact of the elastic deformation of the end case/housing on Axial Piston Machines Cylinder Block/Valve plate lubricating interface", Dresden, pp. 283-294.
- Dhar, S. and Vacca, A. (2015), "A novel FSI-thermal coupled TEHD model and experimental validation through indirect film thickness measurements for the lubricating interface in external gear machines", *Tribology International*, Vol. 82, pp. 162-175.
- Frnaeo, N. (1961), "Pump design by free balance", *Hydraulics & Pneumatics*, Vol. 14 No. 5, pp. 101-107.
- Hashemi, S., Friedrich, H., Bobach, L., Bartel, D., Bobach, L. and Bartel, D. (2017), "Validation of a thermal elastohydrodynamic multibody dynamics model of the slipper pad by friction force measurement in the axial piston pump", *Tribology International*, Vol. 115, pp. 319-337.
- Ivantysynova, M. and Huang, C. (2002), "Investigation of the gap flow in displacement machines considering the Elastohydrodynamic effect", *The Fifth JFPS International Symposium on Fluid Power*, Nara, pp. 219-229.
- Mandal, N.P., Saha, R. and Sanyal, D. (2012), "Effects of flow inertia modelling and valve-plate geometry on swash-plate axial-piston pump performance", *Proceedings of the Institution of Mechanical Engineers, Part I: Journal of Systems and Control Engineering*, Vol. 226 No. 4, pp. 451-465.
- Pan, H.C., Sheng, J.C. and Lu, Y.X. (1989), "Finite difference computation of valve plate fluid film flows in axial piston MachinesInternational", *Journal of Mechanical Sciences*, Vol. 31 No. 10, pp. 779-791.
- Pelosi M. and Ivantysynova M., 2009, "A novel thermal model for the piston/cylinder interface of piston machines", FPMC2009 Hollywood, pp. 12-14.
- Rao, S.S. (1982), *The Finite Element Method in Engineering*, Pergamon Press, Oxford.
- Richardson, D., Sadeghi, F., Richard, G., Rateick, R.G., Jr and Rowan, S. (2017), "Experimental and analytical investigation of floating valve plate motion in an axial piston pump", *Tribology Transactions*, Vol. 60 No. 3, pp. 537-547.
- Shang L. and Ivantysynova M. (2016), "An investigation of design parameters influencing the fluid film behavior in Scaled Cylinder Block/Valve Plate Interface", Florianópolis, SC, pp. 1-10.
- Tang, H.S., Ren, Y. and Xiang, J.W. (2017), "A novel model for predicting thermoelasto-hydro-dynamic lubrication characteristics of slipper pair in axial piston pump", *International Journal of Mechanical Sciences*, Vols 124/125, pp. 109-121.
- Thiagrajan, D., Dhar, S. and Vacca, A. (2015), "A novel fluid structure interaction-EHD model and optimization procedure for an asymmetrical axially balanced external gear machine", *Tribology Transactions*, Vol. 58 No. 2, pp. 274-287.
- Xu, B., Chao, Q., Zhang, J.H. and Chen, Y. (2017a), "Effects of the dimensional and geometrical errors on the cylinder block tilt of a high-speed EHA pump", *Meccanica*, Vol. 52 No. 10, pp. 2449-2469.
- Xu, B., Hu, M., Zhang, J.H. and Mao, Z.B. (2017b), "Distribution characteristics and impact on pump's efficiency of hydro-mechanical losses of axial piston pump over wide operating ranges", *Journal of Central South University*, Vol. 24 No. 3, pp. 609-624.
- Yamaguchi, A. (1966), "Pressure distribution on valve plate of axial plunger pumps and motors", *Seisankenkyu*, Vol. 9 No. 34, pp. 18-20.
- Yamaguchi, A. (1984), "Characteristics of fluid film between a valve plate and a cylinder block of axial piston pumps and motors", *Japan Hydraulic Pneumatic Society*, Vol. 15 No. 4, pp. 314-322.
- Yang, L.J., Nie, S.L., Yin, S., Zhao, J.B. and Yin, F.L. (2015), "Numerical and experimental investigation on torque characteristics of seawater hydraulic axial piston motor for underwater tool system", *Ocean Engineering*, Vol. 104, pp. 168-184.

About the author

Zhanling Ji received PhD in Mechanical Engineering in July 2016 from Beihang University, Beijing. During the study, she carried out the research studies on thermal-structure coupling analysis for a satellite and thermal-fluid-structure coupling analysis for a pump of an electrohydrostatic actuator. Since July 2016, she is a Postdoctoral Fellow and has been working for the multi-disciplinary coupling of high-speed trains, including aerodynamics, multi-body dynamics and structural mechanics. Zhanling Ji can be contacted at: 149018663@qq.com

For instructions on how to order reprints of this article, please visit our website:

www.emeraldgroupublishing.com/licensing/reprints.htm

Or contact us for further details: permissions@emeraldinsight.com